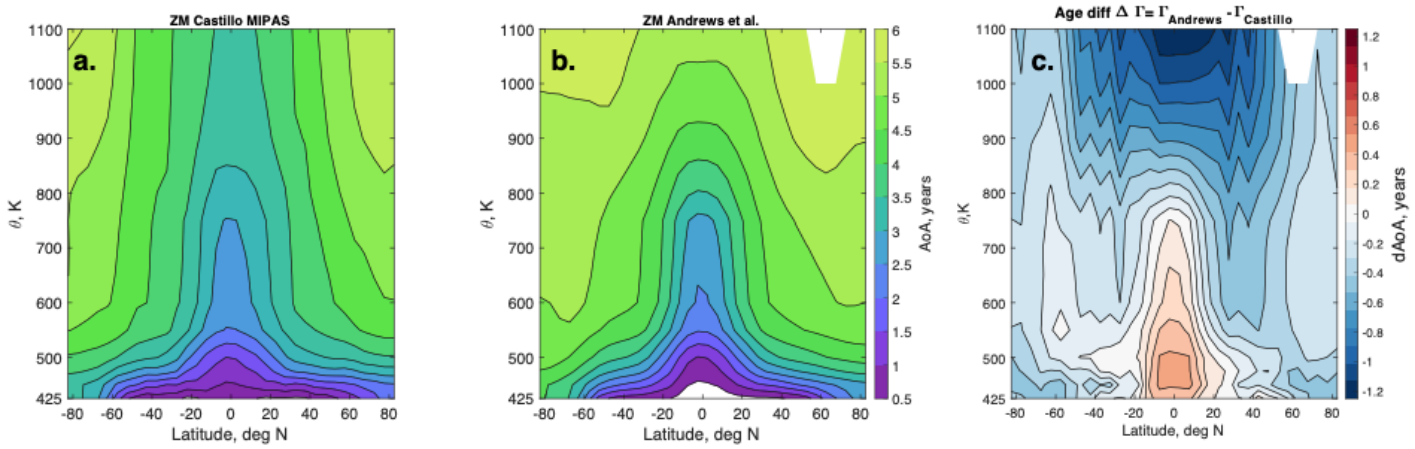

S1: (a) Multi-year mean N_2O-age from MLS v5 N_2O dataset using latitude-varying SF_6-age: N_2O relationships from MIPAS, applied from January 2005 to December 2012. (b) Multi-year zonal mean N_2O -age from MLS v5 N_2O dataset, using empirical CO_2-age: N_2O relationship from Andrews et al., (2001), from 2005-2012. Age contours are scaled by half a year. (c) Absolute age difference between ages obtained using Andrews et al. relationship (b) and MIPAS relationships (a) on the MLS MLS v5 N_2O data from January 2005-December 2012.

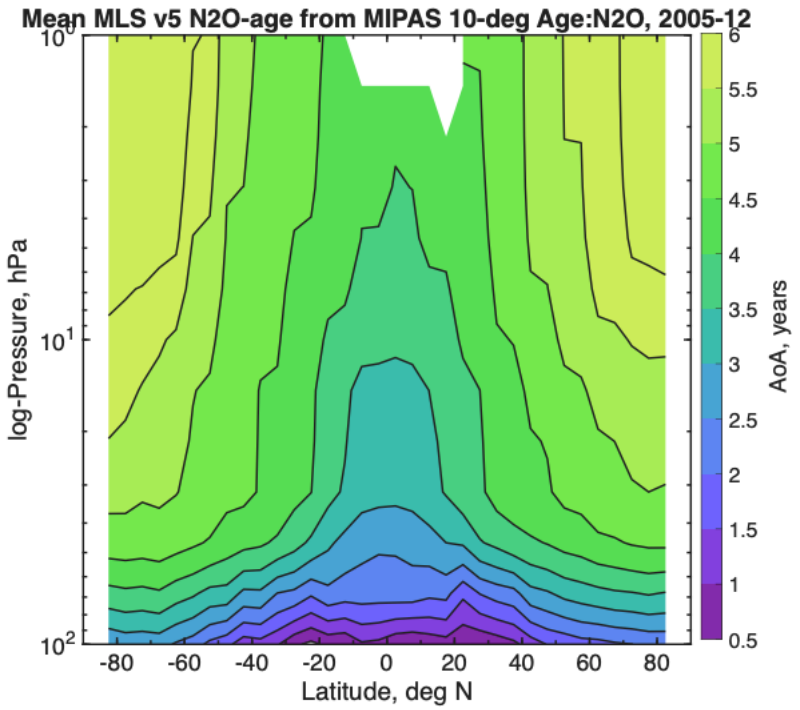

S2: Multi-year mean N_2O -age from MLS v5 N_2O dataset using 10-degree resolved SF_6-age: N_2O relationships from MIPAS, applied from January 2005 to December 2012. Mean age is a function of latitude and height (log-P). Colorbar values are in increments of half a year. Data are from MLS v5 N_2O.

Because of sparse sampling in the mixing regions, the SF_6 -mean ages were consequently sporadic and incomplete, with significant amount of variability. Another motivation for smoothing Age:N_2O relationships arose from deriving N_2O-age (methods described in Section 4.2) using the 10° relationships from Section 3.3.1 The resulting N_2O-age isopleths were jagged, and they did not reflect N_2O-abundances, as seen in Fig. 2, just outside of the tropics and mixing regions (20°-40°).

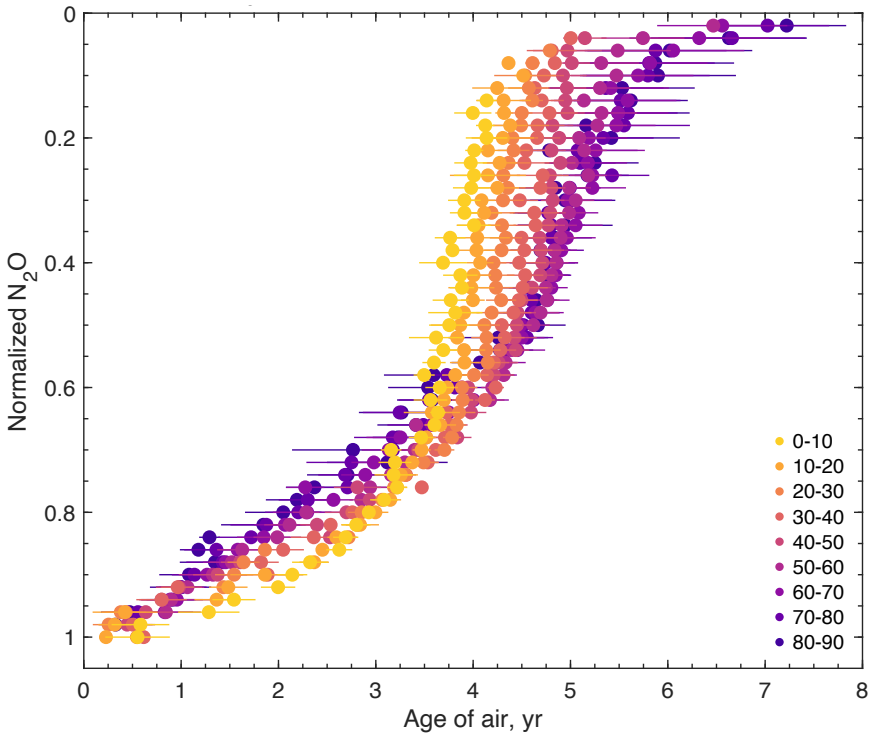

S3: Mean SF_6-age versus normalized N_2O with a latitude resolution of 10-degrees in the SH from 2005-2012. The solid circles represent the mean age for 0.02 bins of normalized N_2O, with error bars indicating 1 standard deviation. Lighter, warmer colors (yellow and orange) represent lower latitudes, while darker, cooler colors (magenta and purple) represent higher latitudes. Data are from MIPAS V5R_224 and V5R_225 N_2O and SF_6 observations.

We compute 27 latitude varying SF_6 -age:N_2O relationships using 36 latitude bins or 5-degree resolved MIPAS mean N_2O and SF_6 -age from 90°S to 90°N (with 87.5°S to 87.5°N being the midpoints). The product is centered at the equator, with 13 individual relationships in each hemisphere. These 27 relationships consist of 5-degree resolved N_2O and SF_6 -age data overlapping multiple latitude bins that are then translated to 36 latitude bins corresponding to the indexing.

Since observations are sparse, we conglomerated data in both hemispheres from 0° to 40. We address this in the deep tropics using observations from 4 different latitude bins in the NH and SH to create a singular relationship to represent the deep tropics (15°S-15°N) because we expect minimal mixing within the tropical pipe region as observed because we expect minimal mixing within the tropical region. The subtropics are also complicated in that there are gaps that result in incomplete relationships as seen in Fig. 6c. We mitigate this by indexing data in a different way, and so we derive relationships over overlapping bins from 10° to 40° while leaving relationships from 45° to 90° intact. Despite the different approach to indexing, the Age:N_2O relationships are conserved.

Since observations are sparse, we conglomerated data in the deep tropics using observations from 4 different latitude bins in the NH and SH to create a singular relationship to represent the deep tropics. In particular, SF_6-age and N_2O observations were used from -15°S to 5°S and 5°N to 15°N (where midpoints are -12.5°S:-7.5S and 7.5°N:12.5°N) to compute a single relationship. We negate two 0°-5° bins in both NH and SH due to sparse sampling and biased older ages. A single relationship is thus applied to 4 bins spanning 15°S to 15°N (bin size of 20°).

The subtropics are also complicated in that there are gaps that result in incomplete relationships as seen in Figure 6c. We mitigate this by indexing data in a different way, and so we derive relationships over larger and overlapping bins in two ways: (1) in the deep-subtropics (10°-25°) and (2) the mixing regions (20°-40°). Data slightly overlap because (1) and (2) are in regions of along isentropic mixing. Before computing mean SF_6-age as a function of N_2O, we sort data in specific latitude bins in the NH and SH. For (1), we sort SF_6-age and N_2O data between 15°-25° (bin size of 10°) to represent the 15°-20° latitude bin, and then for (2), we sort data between 10°-20° (bin size of 10°) to represent the 10°-15° bin, and so we have 2 unique relationships for each hemisphere (or 4 unique relationships).

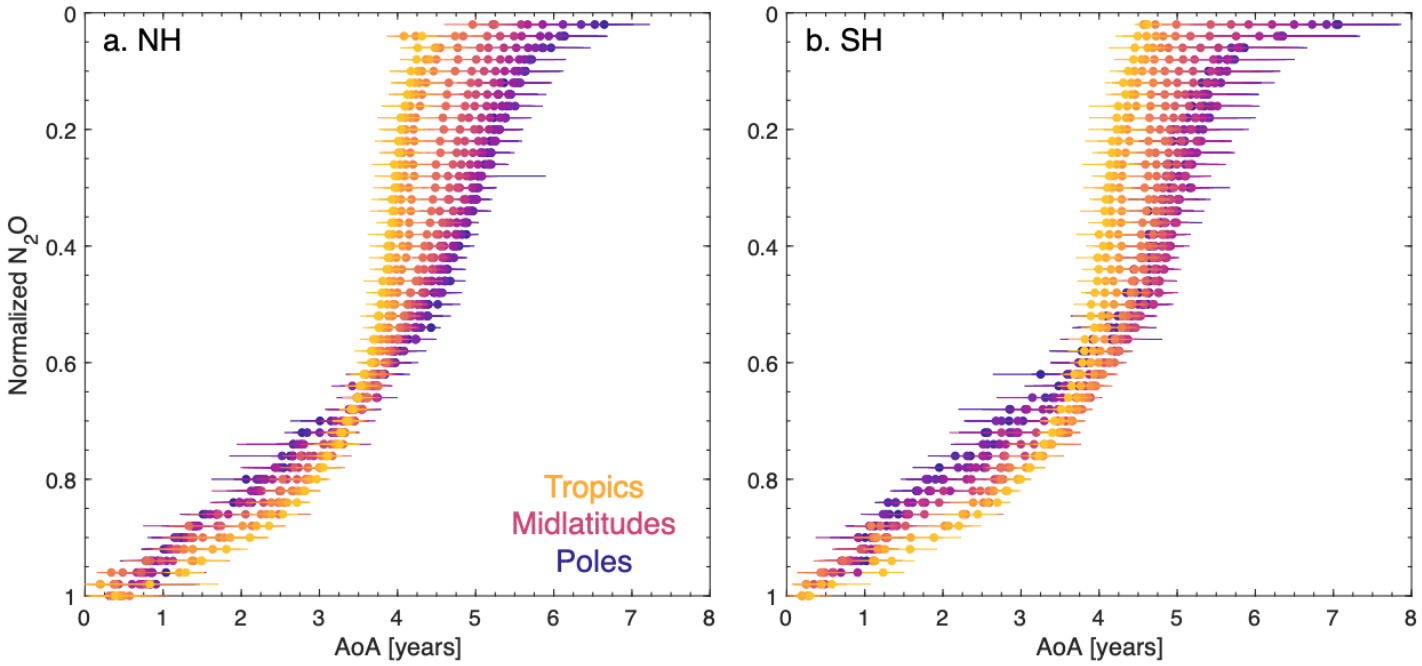

S4: Mean SF_6-age versus normalized N_2O with a tropics coarse latitude resolution in the (a) NH and (b) SH from 2005-2012. The solid circles represent the mean age for 0.02 bins of normalized N_2O, with error bars indicating 1 standard deviation. Lighter, warmer colors (yellow and orange) represent lower latitudes, while darker, cooler colors (magenta and purple) represent higher latitudes. Data are from MIPAS V5R_224 and V5R_225 N_2O and SF_6 observations.

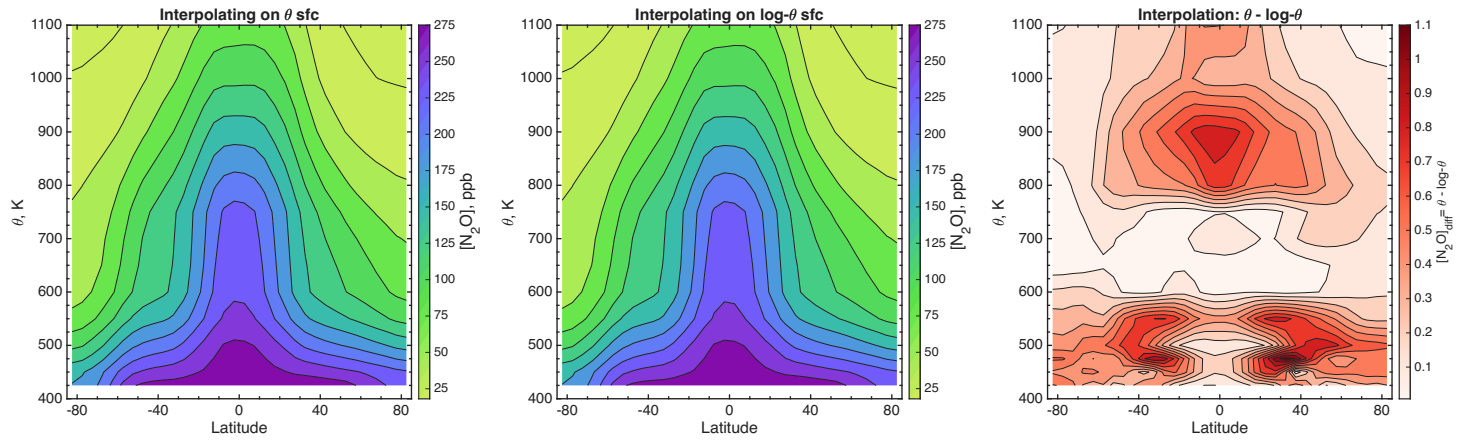

S5: N_2O concentrations plotted as a function of latitude and with potential temperature (theta) as the height coordinate from 2005-2012. a) N_2O interpolated on a constant theta surface; b) N_2O interpolated on a log-theta surface; c) the absolute difference of interpolation methods of a) – b). For a) and b) contours and colorbars are in increments of 25 ppb ranging from 25 - 275ppb and c) contours and colorbar in increments of 0.1ppb ranging from 0.1 to 1.1ppb in ppb. Theta surfaces range from 400K to 1100K. Data are from MLS v5 N_2O.

The advantage of using θ is that it naturally separates mixing from slow meridional transport so the relationships should be clearer. Deriving age as a function of latitude and θ is useful for eventual overturning circulation calculations, as discussed in Equation 1, where the strength of the stratospheric circulation is related to the mass flux of the atmosphere through a given θ surface. Certain judgments were made to enable future calculations of the overturning mass flux of the BDC for future quantitative conclusions on age differences, age gradients, and their relation to circulation strength.

In addition, the rationale for using log-θ surfaces is that this coordinate system considers the mass of the atmosphere, where atmospheric pressure, or mass, exponentially decreases with increasing altitude. The difference of N_2O interpolation on log-θ or θ differed by no more than 1.1 ppb, a difference comparable to that of satellite observation variability.

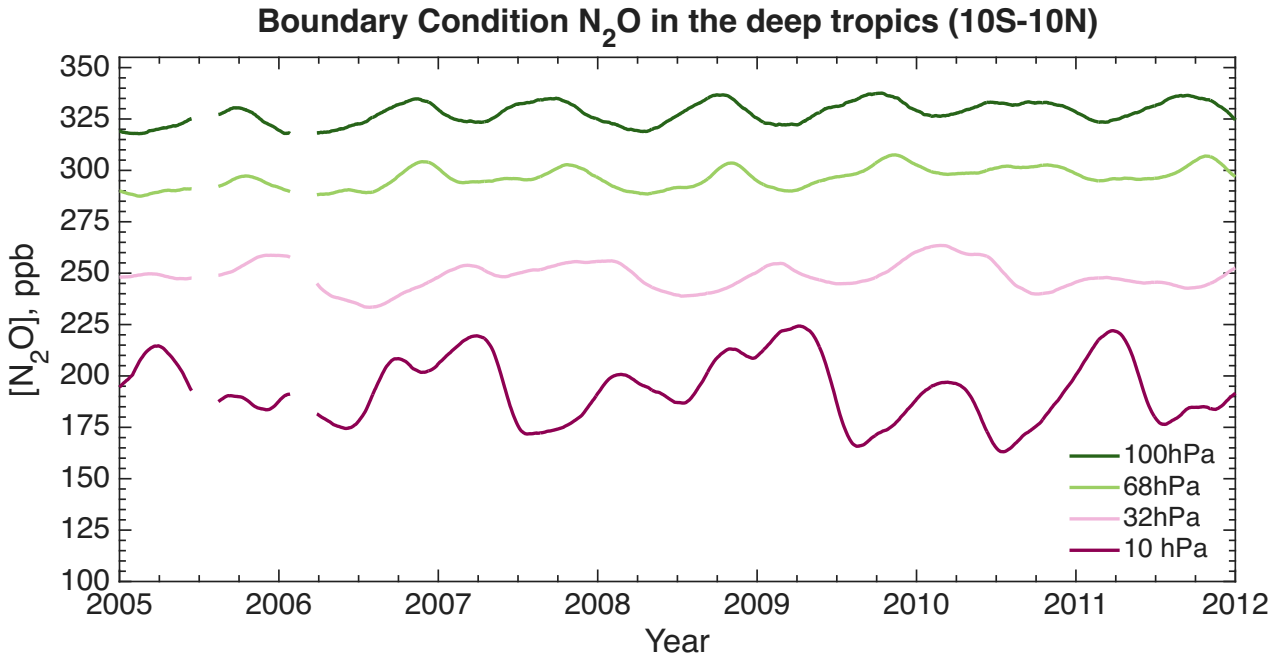

S6: Time series of 60 day running mean of maximum N_2O concentrations measured by MLS in the deep tropics on constant pressure heights from 2005-2015 at 100hPa (dark green), 68hPa (light green), 32hPa (light pink) and 10hPa (magenta). Data are from MLS v5 N_2O.

We want to take a note that the MLS drift is not constant in both height and time. In addition, there is seasonality signature that is significantly exaggerated, even with the ~2-month smoothed mean applied from 100hPa to 32hPa, and particularly at 10hPa in S6. Given the non-linear distribution of the MLS 'seasonality' in the deep tropics (as seen in Figure 1), we acknowledge that the normalization does not filter out this variability uniformly, which has inherent impacts on age derivations.

In Figure 1, maximum tropical N_2O concentrations vary from ~320-340 ppb throughout the timeseries. The minimum values would result in biased older age derivations while higher concentrations would result in younger age derivations. While not perfect, normalizing in the deep tropics – on each daily time stamp – scales the varying maximum values on the same scale, thus filtering out the unrealistic variability signature that is not physically observed.

We find the results to capture the overall structure of the circulation despite these caveats (e.g., Figure 10): 700K is below the strong variability observed in this figure (10hPa) and results at 450K are above 100hPa (the red line plotted in Figure 1).

The results here further motivate the need to use a more accurate product that filters out these signatures and biases.